Polymorphism, superheating, and amorphization of silica upon shock wave loading and release

Sheng-Nian Luo[1] and Thomas J. Ahrens

Lindhurst Laboratory of Experimental Geophysics, Seismological Laboratory, California Institute of Technology, Pasadena, California, USA

Paul D. Asimow

Division of Geological and Planetary Sciences, California Institute of Technology, Pasadena, California, USA

Received 21 November 2002; revised 12 May 2003; accepted 23 May 2003; published 10 September 2003.

[1] We present a detailed and quantitative examination of the thermodynamics and phase change mechanisms (including amorphization) that occur upon shock wave loading and unloading of silica. We apply Debye-Grüneisen theory to calculate both the Hugoniot of quartz and isentropic release paths. Quartz converts to stishovite (or a stishovite-like phase) between 15 and 46 GPa, and persistence of the solid phase above its liquidus (i.e., superheating) is confirmed between 77 and 110 GPa. Calculations compare favorably to measurements of shock and post-shock temperatures. For silica, the method of measuring post-shock temperature is insensitive to predicting whether phase transitions actually occur during release. Measurements of release states in pressure-particle velocity space are compared to computed frozen-phase release paths. This comparison suggests transformation of a stishovite-like phase to lower density phases including quartz, liquid, or dense amorphous glass. Transformations to liquid or glass occur upon release from peak pressure of 26 GPa and above. The isentropic release assumption appears to be approximately valid. A shock pressure-temperature scale relating metamorphism of silica in shock-loaded quartz is proposed. Neither recovery of coesite nor substantial quantities of crystalline stishovite-like phases upon shock loading of quartz is predicted. Trace amounts of crystalline stishovite-like phases from shock loading between 15 and 26 GPa are expected. *INDEX TERMS:* 3924 Mineral Physics: High-pressure behavior; 3939 Mineral Physics: Physical thermodynamics; 3944 Mineral Physics: Shock wave experiments; *KEYWORDS:* polymorphism, amorphization, superheating, silica, shock wave, release

Citation: Luo, S.-N., T. J. Ahrens, and P. D. Asimow, Polymorphism, superheating, and amorphization of silica upon shock wave loading and release, *J. Geophys. Res.*, *108*(B9), 2421, doi:10.1029/2002JB002317, 2003.

1. Introduction

[2] Silica is of great importance for geophysics and condensed-matter physics. It is a prototype system for understanding the fundamental physics of phase changes, and an end member of silicates believed to be important constituents of the terrestrial planets [*Hemley et al.*, 1994]. The phase change mechanisms and kinetics upon dynamic loading and subsequent release in laboratory impact and intense laser irradiation experiments are also of particular interest. Shock wave loading and unloading induce interesting phenomena such as polymorphism, superheating, amorphization upon compression and decompression, and shear melting. Models of material behavior under dynamic loading/unloading are also required for interpreting the effect of natural planetary impacts, yet the existing quartz shock pressure-temperature ($P - T$) scale [*Stöffler*, 1971] was based on earlier calculations [*Wackerle*, 1962] that did not take the quartz-stishovite transition explicitly into account. Previously, considerable efforts have been made to address shock loading and release behavior of silica [*Ahrens and Rosenberg*, 1968; *Ahrens et al.*, 1969; *Grady et al.*, 1974; *Podurets et al.*, 1976; *Chhabildas and Grady*, 1984; *Chhabildas and Miller*, 1985; *Sekine et al.*, 1987; *Swegle*, 1990; *Ng et al.*, 1991; *Boettger*, 1992; *Langenhorst et al.*, 1992; *Akins and Ahrens*, 2002]. For example, the effect of phase change of quartz on wave propagation has been studied [*Grady et al.*, 1974; *Swegle*, 1990], and related thermodynamics was partly discussed [*Swegle*, 1990]. *Boettger* [1992] constructed an α-quartz-stishovite transformation model assuming phase equilibrium is approached. As experiments demonstrate that the onset of such a transition occurs where the shock pressure (13–15 GPa) is higher than the equilibrium pressure ($\sim$7.5 GPa [*Ahrens*

[1]Now at Plasma Physics, Los Alamos National Laboratory, Los Alamos, New Mexico, USA.

0148-0227/03/2002JB002317$09.00

and Gregson, 1964]), we do not assume phase equilibrium in the present work. A complete quantitative description of the thermodynamic states of quartz upon shock wave loading and release is of great interest but not well established. Previously, the constraints on the phases upon release imposed by post-shock temperature measurements [*Boslough*, 1988], have not been completely explored. Moreover, the validity of the isentropic assumption for converting pressure-particle velocity ($P - u_p$) data (measured by *Podurets et al.* [1976]) into pressure-volume ($P - V$) paths along release adiabats involving phase changes, has been questioned by these authors.

[3] Silica polymorphs have been extensively investigated with dynamic techniques, and the shock wave equations of state (Hugoniots) of fused quartz, α-quartz, coesite and stishovite are well defined [*Wackerle*, 1962; *Al'tshuler et al.*, 1965; *Trunin et al.*, 1971; *Podurets et al.*, 1981; *Marsh*, 1981; *Luo et al.*, 2002a]. Shock temperature measurements [*Lyzenga et al.*, 1983] on fused quartz and on quartz extended the melting curve of silica beyond the pressure-temperature range of existing diamond-anvil cell experiments [e.g., *Shen and Lazor*, 1995]. The phase diagram of silica has been established up to megabar pressure regime based on the joint efforts from static and dynamic experiments, and theoretical simulations such as *ab initio* [*Karki et al.*, 1997] and molecular dynamics techniques [*Luo et al.*, 2002b]. The unloading paths of shocked quartz were measured in $P - u_p$ space but have not been fully utilized [e.g., *Podurets et al.*, 1976]. These advances in knowledge of the equation of state and other thermodynamic properties of silica (especially stishovite) now permit a detailed quantitative examination of thermodynamic state and mechanisms of phase changes upon shock wave loading and unloading, as well as post-shock temperature measurement and isentropic release assumption.

[4] The issue of whether crystalline stishovite or rather a dense amorphous phase forms at high pressure along the quartz Hugoniot has been controversial. Recently, *Panero et al.* [2003] proposed that an amorphous phase is present on the Hugoniot, using room temperature diamond-anvil cell $P - V$ data and a thermal correction to obtain a constructed Hugoniot $\sim$2% denser than that observed. However, *Akins and Ahrens* [2002] and *Akins* [2003], using the same shock wave data and formulation with the same parameters, failed to reproduce the result of this calculation and concluded that the measured Hugoniot states represent stishovite and other high-pressure phases. Direct structural data, for example, by transient X-ray diffraction in the shock state [*Loveridge-Smith et al.*, 2001] is needed to resolve this issue. In the meantime, lacking direct evidence bearing on the crystallinity of the Hugoniot state, we only show in this work that the thermal equation of state of the shock-state phase is indistinguishable from that of stishovite. Furthermore, some studies arguing for an amorphous Hugoniot state have, in our view, assumed too much from examination of shock-recovered material [*Gratz et al.*, 1992; *Sharma and Sikka*, 1996; *Fiske et al.*, 1998]. This paper shows how crystalline stishovite (or stishovite-like) phase, if formed, would be very difficult to recover without special treatments. Non-negligible amount of stishovite (and other crystalline phases such as Fe_2N-type) was recovered from shocked quartz along with large amount of an amorphous phase [*De Carli and Milton*, 1965; *Kleeman and Ahrens*, 1973; *Sekine et al.*, 1987]. This fact could support that crystalline stishovite-like phase forms on Hugoniot (while it cannot rule out the possibility of amorphization upon shock loading). Several post-stishovite phases have been proposed from dynamic recovery and static experiments, including $CaCl_2$, α-PbO_2 and $P2_1/c$ structures [*Cordier et al.*, 1993; *Dubrovinsky et al.*, 2001; *Haines et al.*, 2001; *Dera et al.*, 2002; *Murakami et al.*, 2003]. While the exact phase produced on Hugoniot is subject to debate, its bulk properties are expected to be stishovite-like [*Luo et al.*, 2002a, 2002b; *Akins and Ahrens*, 2002]. In the following discussions, stishovite does not necessarily refer to rutile structure literally; instead, it should be regarded as stishovite-like.

[5] We begin by reviewing the methodology of calculating both Hugoniot states and release isentropes in both single-phase and mixed-phase states using Debye-Grüneisen theory. For release, we examine the frozen and non-frozen phase release paths and their relation to the phase diagram of silica and measurements of $P - u_p$ upon release. On the basis of calculated thermodynamic states and phase assemblages upon shock loading and unloading, we discuss superheating, melting, polymorphism, and amorphization in silica. We also evaluate the validity of the isentropic assumption for mixed-phase and reacting release paths. Finally we establish a revised shock $P - T$ scale for impact events involving quartz.

2. Thermodynamics of Quartz Upon Shock Wave Loading and Release

2.1. Formulation for Single-Phase Properties

[6] To determine the complete thermodynamic state upon shock wave loading (Hugoniot) and release paths, we will adopt classical Debye-Grüneisen theory. The detailed derivations can be found in the literature [*Morse*, 1964; *Swegle*, 1990]. For the convenience of the reader and because of some typographical errors in previous work, we will briefly review the physics and list the equations needed. For non-metal materials under the pressure and temperature conditions of interest, we need only consider the lattice contribution to specific heat (C_V) and neglect electronic contribution. The Grüneisen parameter (γ) is assumed to be an explicit function of volume V only (specific volume $V = 1/\rho$ where ρ is density). From Debye theory,

$$C_V(T, V) = C_{vm}\left[4D\left(\frac{\theta}{T}\right) - \frac{3\theta/T}{e^{\theta/T} - 1}\right], \tag{1}$$

where

$$D(x) = \frac{3}{x^3}\int_0^x \frac{y^3 dy}{e^y - 1} \tag{2}$$

is the Debye function. C_{vm} is the Dulong-Petit high-temperature limit of C_V, i.e., normally $3R$ per gram-atom for solids where R is the gas constant. Here θ is Debye's temperature at corresponding V, and is related to T-independent γ as

$$\gamma(T, V) = \gamma(V) = -\frac{\mathrm{d}\ln\theta}{\mathrm{d}\ln V}. \tag{3}$$

Thus, given $\gamma(V)$,

$$\theta(V) = \theta(V_0)\exp\left\{-\int_{V_0}^{V}\frac{\gamma(v)}{v}dv\right\}, \quad (4)$$

where subscript 0 denotes the reference state, normally standard temperature, and pressure (STP). By thermodynamic integration, we can obtain entropy S, P, and internal energy E as

$$S(T,V) = S(T_0,V_0) + C_{vm}\left\{\frac{4}{3}\left[D\left(\frac{\theta}{T}\right) - D\left(\frac{\theta_0}{T_0}\right)\right] - \ln\left(\frac{1-e^{-\theta/T}}{1-e^{-\theta_0/T_0}}\right)\right\}, \quad (5)$$

$$P(T,V) = P(T_0,V) + \frac{\gamma C_{vm}}{V}\left[TD\left(\frac{\theta}{T}\right) - T_0 D\left(\frac{\theta_0}{T_0}\right)\right], \quad (6)$$

$$E(T,V) = E(T_0,V_0) - \int_{V_0}^{V}P(T_0,v)dv + C_{vm}\left[\frac{1}{3}A(\theta,T_0) + TD\left(\frac{\theta}{T}\right)\right], \quad (7)$$

where

$$A(\theta,T) = T\left[D\left(\frac{\theta}{T}\right) - 3\ln\left(\frac{1-e^{-\theta/T}}{1-e^{-\theta_0/T_0}}\right) - 4D\left(\frac{\theta_0}{T_0}\right)\right]. \quad (8)$$

The expressions for enthalpy H, Helmholtz free energy F, and Gibbs free energy G can be readily obtained from the definitions $H = E + PV$, $F = E - TS$ and $G = F + PV$. Thus, given two of the thermodynamic quantities, for a single phase the complete thermodynamic state can be determined.

[7] $P(T_0, V)$, $\gamma(V)$, and associated parameters are assumed to be known a priori. The cold pressure $P(T_0, V)$ is most available at T_0 = 300 K, in the form of finite-strain Birch-Murnaghan or Vinet universal equation of state (EOS) [*Cohen et al.*, 2000]. For third-order Birch-Murnaghan EOS,

$$P(f) = 3K_{T0}f(1+2f)^{\frac{5}{2}}\left[1 + \frac{3}{2}\left(K'_{T0} - 4\right)f\right], \quad (9)$$

where the Eulerian strain $f = \frac{1}{2}\left[(V/V_0)^{-2/3} - 1\right]$ and K_{T0} and K'_{T0} are the ambient isothermal bulk modulus and its pressure derivative, respectively. A common expression for $\gamma(V)$ is

$$\gamma/\gamma_0 = (V/V_0)^q, \quad (10)$$

although it could be written in a more general form to accommodate cases of extreme compression and expansion [*Swegle*, 1990]. The reference values S_0 and E_0 at STP for various phases of SiO_2 are available in the literature [*Robie et al.*, 1978; *Saxena et al.*, 1993; *Malcolm*, 1998]. E_0 for quartz is arbitrarily chosen as 0, and other phases are referenced to quartz. The Debye temperature at STP, θ_0, can be determined from elastic constants (acoustic θ) [*Anderson*, 1963] or fitting to specific heat C_V (thermal θ). In our calculations, the latter value is adopted. With the fitted values of θ_0 [*Swegle*, 1990], we calculated entropy as a function of temperature at ambient pressure for quartz and stishovite (Figure 1). The values from the Debye-Grüneisen theory are in good agreement with tabulated handbook values [*Robie et al.*, 1978; *Saxena et al.*, 1993]. We take this as indication that the Debye-Grüneisen theory, though approximate, is adequate for our purposes. Table 1 lists the input parameters needed for the calculation of complete thermodynamic states of quartz and stishovite. We also included static yield strength Y of quartz. The strength effect of quartz at high pressures is still under debate, and we will correct the measured peak stress (σ_H) for strength. Note that this correction is not crucial, as it will not affect the results significantly. Because of the apparently subtle thermomechanical and energetic differences between stishovite and post-stishovite phases, we will make no distinction between these two [*Luo et al.*, 2002b] in the shock loading/unloading calculations.

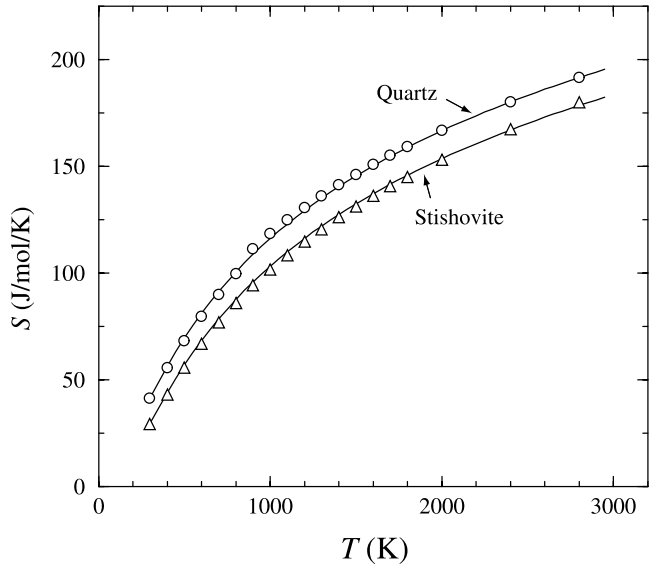

Figure 1. Entropy (S) of quartz and stishovite as a function of temperature (T) at ambient pressure. Symbols, *Saxena et al.* [1993]; solid curves, calculations from Debye-Grüneisen theory.

2.2. Treatment of Two-Phase Aggregates

[8] If a phase change occurs along the Hugoniot or during release, we will assume that only two phases are present at any time. We further assume that the assemblage of the parent and new phases maintains a series of states in (possibly metastable) thermal and mechanical equilibrium; that is, T and P are common to both phases. No heterogeneous equilibrium is assumed (i.e., we do not require G to be equal among phases). Then, in the case of a mixture of phase 1 and 2, the total internal energy, specific volume, and entropy are given by

$$E = (1-\lambda)E_1 + \lambda E_2, \quad (11)$$

$$V = (1-\lambda)V_1 + \lambda V_2, \quad (12)$$

$$S = (1-\lambda)S_1 + \lambda S_2, \quad (13)$$

Table 1. Thermodynamic Parameters for Quartz and Stishovite[a]

	K_0, GPa	K_0'	V_0, cm^3/g	γ_0	q	C_{vm}, J/K/g	θ_0, K	θ_0^{ac}, K	S_0, J/K/g	E_0, J/g	Y, GPa
α-quartz	37.7	6.4	0.3773	0.70	2.0	1.245	999	571	0.69	0.0	4.4
Stishovite	306.0	5.0	0.2331	1.35	2.6	1.245	1037	1190	0.49	777.2	–

[a]Here θ_0 is thermal Debye's temperature, and θ_0^{ac} is the calculated acoustic Debye's temperature at STP. Y: static yield strength. S_0 and E_0 are from *Saxena et al.* [1993]. Other data for stishovite are from *Luo et al.* [2002a], and for quartz, *Swegle* [1990].

where λ is the mass fraction of phase 2. Each phase is assumed to be relaxed to its own homogeneous equilibrium equation of state. For $i = 1, 2$, $S_i = S_i(P, T)$, $E_i = E_i(P, T)$, and $V_i = V_i(P, T)$ satisfy equations (5)–(7) with appropriate parameters (Table 1). For mixtures of two phases, we now need to specify three independent variables to constrain the complete state of the system. For Hugoniot state calculations we take P, E, and V from the Rankine-Hugoniot conservation equations and solve equations (5), (11), (12) and (13) iteratively to obtain T, S, and λ. For frozen-phase release calculations we take fixed P, S, and λ, in which case we can solve to obtain T and V. Finally, for release paths where we have obtained a $P - V$ path as explained below, we can relax the assumption of fixed λ and at fixed P, S, and V we solve to obtain T and λ. Thus the complete thermodynamic state on mixed-phase Hugoniots and certain release paths can be resolved.

2.3. Shock Wave Loading

[9] The Hugoniot of quartz has been previously determined [*Wackerle*, 1962; *Trunin et al.*, 1971; *Marsh*, 1981] as shown in Figure 2, which is assumed to be hydrostatic, and fitted to analytical form for later calculations. We interpret segment M_1M_2 as a mixed-phase regime (quartz and stishovite). Segments QM_1 and M_2S are regarded as pure quartz and stishovite phases, respectively. The exact locations of M_1 and M_2 can be resolved from the value of λ. Using P, V, and $E = E_0 + 1/2(P + P_0)(V_0 - V)$ on the fitted Hugoniot, we solved simultaneously for shock temperature T and the mass fraction of stishovite λ; total shock state entropy S then follows from equation (13). Table 2 lists thermodynamic parameters of shock states at several pressures along the principal Hugoniot of quartz.

[10] The mass fraction of stishovite, λ, starts to increase at 15 GPa and reaches ~1 at 46 GPa (Figure 3); thus the mixed phase regime of quartz and stishovite, M_1M_2, is 15–46 GPa. Along the Hugoniot, as the mass fraction of stishovite becomes appreciable around 23 GPa, T_H (H denotes Hugoniot) increases steeply due to the large decrease of the total volume and concomitant increase in the internal energy. At higher pressures above 23 GPa, T_H increases steadily through the mixed-phase and pure stishovite regimes (Figure 4). This is consistent with the observation that the shock-front instability develops at about 23 GPa [*Zhugin et al.*, 1999]. The shock temperature was independently measured in the range of 70–110 GPa [*Lyzenga et al.*, 1983]. The calculation agrees closely with experiment except calculated values are higher (about 6–8% with experimental errors considered) at pressures of ~100 GPa and above. This could be due to high-temperature heat capacities greater than the $3R$ limit assumed by Debye theory, although larger $\theta(V)$ could partly offset this effect at higher pressures. Stishovite remains the sole Hugoniot state phase up to 110 GPa; comparison to the phase diagram of silica (and stishovite melting curve) obtained from experiments and molecular dynamics simulations [*Luo et al.*, 2002b] (Figure 4) make it clear that superheating does exist between 77 and 110 GPa along the Hugoniot of quartz. Beyond about 110 GPa, stishovite melts as demonstrated by shock temperature [*Lyzenga et al.*, 1983] and sound speed measurements [*Chhabildas and Miller*, 1985].

2.4. Release

[11] The high-pressure phases produced upon shock wave loading, Stishovite or post-stishovite phases, could in principle transform into low pressure/density phases such as quartz and coesite, or become melted or amorphized during release from the peak-state pressure and temperature, depending on the kinetics involved. We make a distinction between the state when the sample is recovered and examined (recovery state, ambient pressure, and temperature) and the post-shock state (ambient pressure and high temperature, denoted as R), because significant phase changes could have occurred during cooling over a time period much longer than the shock loading or unloading duration. Thus the recovered phases are not necessarily the same as those on the release paths.

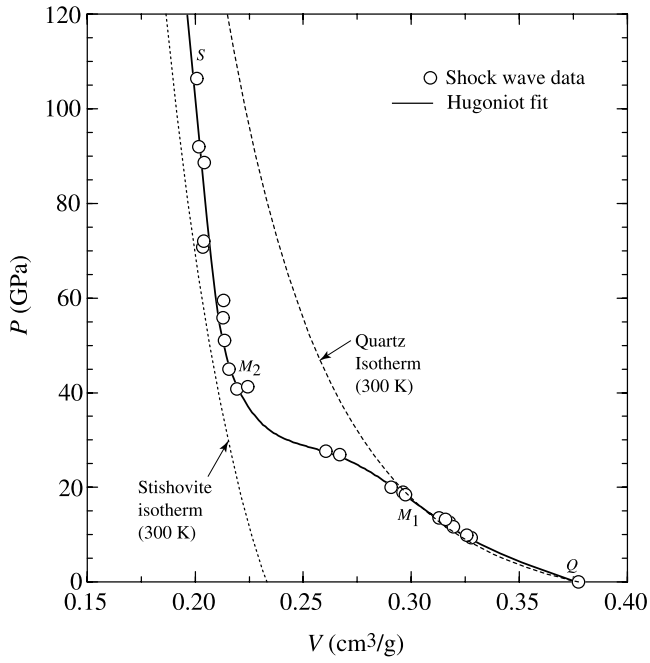

Figure 2. Principal Hugoniot of quartz. Data are from *Wackerle* [1962], *Trunin et al.* [1971], and *Marsh* [1981]. Segments QM_1, M_1M_2, and M_2S are regimes of pure quartz, mixed-phase of quartz and stishovite, and pure stishvoite, respectively. The 300-K isotherms of quartz and stishvoite are from *Swegle* [1990] and *Luo et al.* [2002a].

Table 2. Shock and Post-Shock Temperature of Shocked Quartz: Measurement and Calculation[a]

σ_H, GPa	P_H, GPa	P_H^c, GPa	V_H, cm^3/g	T_H^a, K	T_H^c, K	T_R^b, K	$T_{R,s}^c$, K	S_H, J/K/g
75.9	73.0	73.6	0.2065	4440 ± 40	4425	–	3279	3.365
85.9	83.0	83.3	0.2042	4850 ± 130	5090	3660	3589	3.527
92.5	89.6	90.3	0.2025	5430 ± 120	5535	3920	3756	3.621
99.3	96.4	97.3	0.2009	5630 ± 140	6000	4000	3906	3.712
107.8	104.9	106.0	0.1990	5900 ± 200	6585	–	4048	3.817
109.7	106.8	107.6	0.1987	6100 ± 190	6715	–	4074	3.839

[a]Subscript H: Hugoniot; R, post-shock (ambient pressure); a: *Lyzenga et al.* [1983]; b: *Boslough* [1988]; c: calculation with Debye-Grüneisen theory at given volume. $T_{R,s}$ is obtained assuming frozen-phase release. The σ_H, the experimental uniaxial stress, is corrected to hydrostatic stress (pressure) P_H with $P_H = \sigma_H - \frac{2}{3}Y$.

[12] The post-shock state can be readily calculated if we assume that no phase changes (frozen-phase) occur upon release and that the release is isentropic. It is not impossible that such a frozen path actually occurs, provided appropriate kinetics. At the peak Hugoniot state, the entropy S and phase proportions λ are obtained from the mixed-phase equations in the previous section (e.g., Table 2 and Figure 3) and these values of S and λ are held fixed along the release path to define a frozen-phase isentropic path. Thus at any pressure P along the frozen release path, we solve for T and V as described above. The whole frozen release $P - V - T$ paths from certain peak pressures, including post-shock temperature (T_R), were calculated. On the basis of the shock temperature recordings of *Lyzenga et al.* [1983], *Boslough* [1988] obtained temperatures released from several shock states which were interpreted as post-shock temperatures. Our calculations closely agree with Boslough's results (Table 2 and Figure 4).

[13] Whether phase changes occur upon release can possibly be resolved from well-measured release paths. One common method to determine release states is to measure the particle velocity of the shock states achieved when the shock passes from the sample into a series of buffer materials of lower impedance than the sample (e.g., polycarbonate, polystyrene, compressed Ar) as well as the free surface velocity of the sample material. By shock loading the sample to the same peak pressure and then unloading adiabatically against a series of such lower impedance buffer materials, a sequence of release states in the $P - u_p$ plane is obtained. Figure 5 shows three release paths unloaded from shock states H_1, H_2, and H_3 [*Podurets et al.*, 1976]. In order to transform from the $P - u_p$ to the $P - V$ plane, we assume that the release path is an isentrope. If phase changes occur on release (non-frozen release), this isentropic assumption is under debate [*Podurets et al.*, 1976]. Although independent verification of the isentropic assumption is not available, the assumption itself does not violate any thermodynamic laws. We will assume release to be isentropic in the following discussion.

[14] For isentropic flow, the Riemann invariant [*Zel'dovich and Raizer*, 2002] is

$$J_{\pm} = u_p \pm \int \frac{dP}{\rho C}, \tag{14}$$

where C is speed of sound $\left(C^2 \equiv \frac{dP}{d\rho}|_S\right)$. Thus the volume increase ΔV along release isentrope,

$$\Delta V = -\int_{V_1}^{V_2} \frac{du_p}{dP}|_S \, du_p, \tag{15}$$

can be obtained from the release path in the $P - u_p$ plane. In some cases, only u_p at the free surface and peak shock state are known (point H and R in Figure 5 insert), possibly with a few intermediate states (e.g., B). It can be shown by a variational method [*Lyzenga and Ahrens*, 1978] that the final volume calculated from equation (15) using a piecewise linear fit to a discrete series of $P - u_p$ points is a minimum estimate of the true release volume. $P - u_p$ measurements via other techniques such as reverberation and release-wave profile [*Chhabildas and Miller*, 1985] agree with the $P - u_p$ results from the buffer method [*Podurets et al.*, 1976]. The measured $P - u_p$ paths [*Podurets et al.*, 1976] were fitted to analytical form (Figure 5), and mapped to $P - V$ space as shown in Figure 6.

[15] We may now compare the release paths inferred from conversion of $P - u_p$ data with the isentropic frozen-phase releases. In $P - V$ space (Figure 6), the release paths converted from measured $P - u_p$ can be divided into an initial high-pressure segment that remains close to the frozen-phase calculation followed by a low-pressure seg-

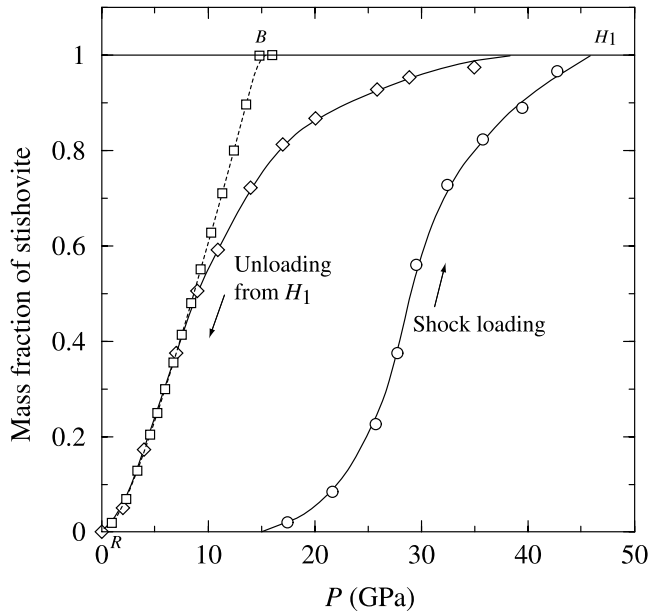

Figure 3. Quartz-stishovite transformation: mass fraction of stishovite λ versus P upon loading, and release from H_1 (peak stress of 48.5 GPa). Symbols are points of calculation. From the mass fractions on loading path (circles), the mixed-phase regime on Hugoniot is 15–46 GPa. Release paths H_1R (diamonds) and H_1BR (squares) follow the corresponding $P - V$ paths in Figure 6a (also see text).

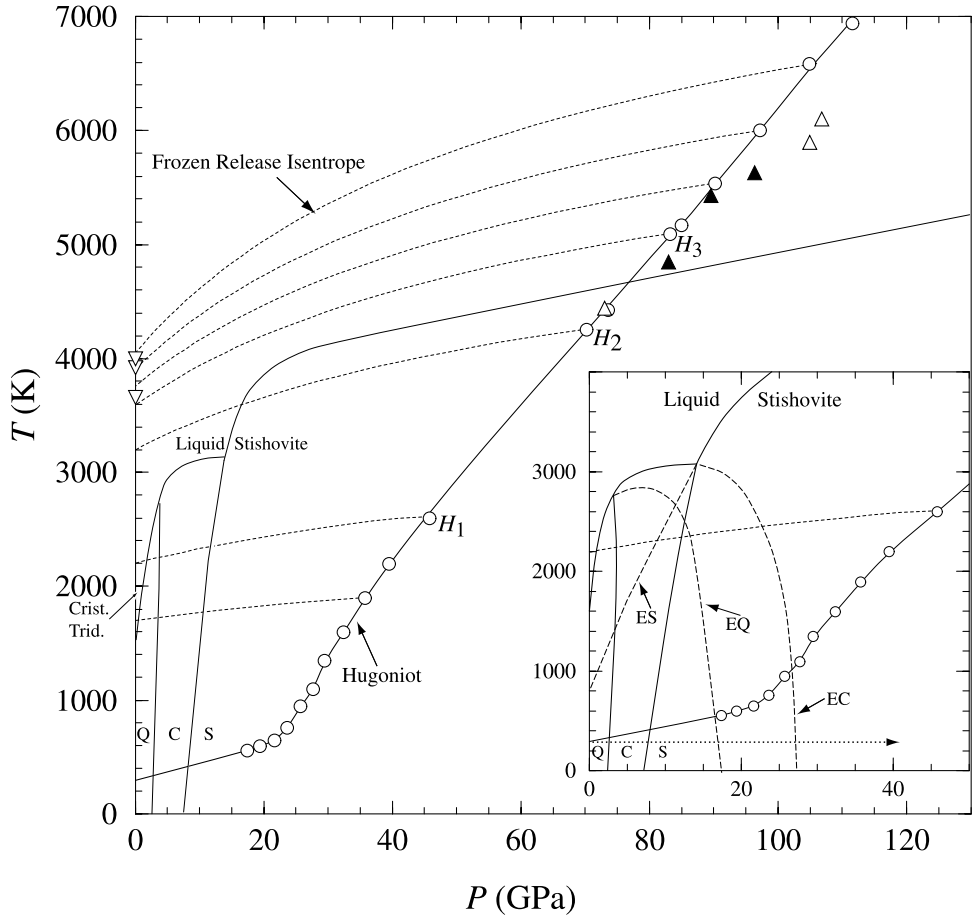

Figure 4. Phase diagram of silica [*Luo et al.*, 2002b], calculated quartz-Hugoniot temperature (circles), measured shock temperature (solid and open triangles) [*Lyzenga et al.*, 1983] and post-shock temperature (inverted triangles, released from shock states denoted as solid triangles) [*Boslough*, 1988]. Dashed curves are frozen-phase release isentropes. Q: quartz, C: coesite, and S: stishovite. H_1, H_2, and H_3 denote three typical states on Hugoniot. Note that the slope of $T(P)$ in stishovite regime is not significantly shallower than that in mixed-phase regime, as the slope of internal energy $E(P)$ remains large (E can be visualized from Rayleigh line; refer to Figure 2). On the contrary, the slope of $T(P)$ for the principal Hugoniot of stishovite is much shallower. (insert) Same as the full figure except that long dashed curves are fictitious extension (metastable) of melting curve of quartz (EQ), coesite (EC) and stishovite (ES). Dotted line denotes the room temperature static compression path, where quartz and coesite become amorphous at 25–35 GPa [*Hemley et al.*, 1988].

ment beginning near ~30 GPa that deviates considerably towards higher volume. This indicates that stishovite transforms to lower density phases. The post-shock density ρ_R released from low (H_1) and high (H_3) pressure are 2.29 and 2.14 g/cm^3, respectively (both close to glass density at STP 2.20 g/cm^3). In the case of intermediate pressure H_2, ρ_R is considerably denser (3.01 g/cm^3, Table 3). This result could be due to differences in the identities and proportions of the phases that form upon release from these three states, or perhaps to differing degrees of relaxation if a glassy phase is involved. The production of lower density, higher entropy phases such as quartz and glass (or melt) during release does not necessarily mean that the final temperature is significantly lower than that from frozen phase release, because the entropy of fusion of silica is small and the smaller γ_0 of low density phases would partly offset the temperature decrease induced by endothermic phase transition and volume expansion. Indeed the differences between T_R estimated for frozen-phase releases and releases with phase transitions are in the range 100–350 K (Table 3), or comparable to the error in post-shock temperature measurements.

[16] Amorphous phases are readily recovered from shocked quartz (e.g., *Wackerle* [1962]), but this does not necessarily imply significant amorphous material at the post-shock state R, since amorphization or melting might occur afterwards. However, the appreciable decrease in density shown in $P - V$ paths converted from measured $P - u_p$ paths clearly demonstrates such phase changes do occur along release paths (Figure 6, Table 3). The thermodynamic paths upon frozen-phase release are different for H_1, H_2 and H_3; that is, different phase changes are supposed to be triggered at distinct equilibrium phase boundaries (Figure 4). Along frozen release path H_1, stishovite remains stable until it crosses the coesite-stishovite boundary at 12 GPa and other phase boundaries below 5 Gpa; thus we might expect to see the transition of stishovite to coesite, β-quartz, and liquid in

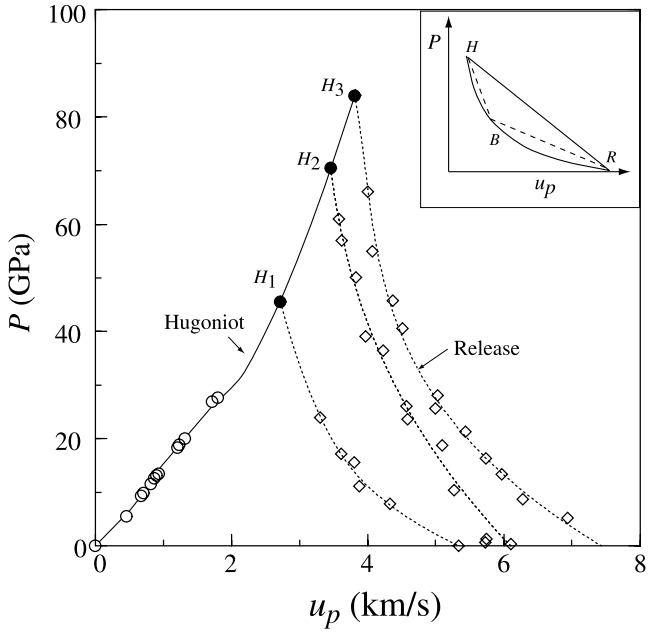

Figure 5. Measured $P - u_p$ upon shock loading and release: open circles, *Wackerle* [1962]; solid circles and diamonds, *Podurets et al.* [1976]. (insert) Schematic release paths in $P - u_p$. H, B, and R denote shock, intermediate, and final release states, respectively. Solid curve HBR denotes the real release path, solid line HR is an approximated release path with u_p known only at H and R, and dashed lines HBR with u_p known only at H, B, and R.

sequence. For H_2, stishovite remains stable until the liquid-solid phase boundary is crossed at 16 GPa, where stishovite may melt. The release from H_3 is different in that the shock state (as well as the whole frozen release path) is superheated; thus melting could occur at any point on the release path. The $P - V$ paths converted from $P - u_p$ [*Podurets et al.*, 1976] assuming isentropic release (H_iR, i = 1, 2, and 3, Figures 6a, 6c, and 6d) in fact differ significantly both from the frozen-phase release calculations (H_iR' in Figure 6) and from these predicted thermodynamic equilibrium paths. The deviations are significant even when we take into account the errors in estimation of the release paths (about 6%, according to *Chhabildas and Grady* [1984]). On release from H_1, for example (Figure 6a), the phase should remain stishovite until 12 Gpa, yet H_1R begins to deviate from H_1R' at about 30 GPa and is significantly different by 20 GPa. Likewise, release from H_2 deviates from the frozen phase path before encountering any phase boundaries (Figure 6c). The most plausible explanation for this curious behavior, if the $P - V$ paths converted from $P - u_p$ are accurate, is that non-hydrostatic stresses may displace the equilibrium boundaries to higher pressure [e.g., *Simha and Truskinovksy*, [1994]. Release from H_3, on the other hand, deviates in the sense that a phase transition is delayed relative to crossing the equilibrium boundary (Figure 6d), which can be explained by the kinetics of superheating of crystalline phases in liquid stability fields [*Luo et al.*, 2002c]. There is also the possibility of artifacts resulting from fitting smooth curves through series of discrete $P - u_p$ points that are not densely sampled enough to capture sharp changes in slope at phase boundaries, though such breaks are not obvious in the $P - u_p$ data (Figure 5).

[17] Since the data suggest that phase transitions do occur during release, we formulate a method for computing isentropic release with phase changes. We assume that the total entropy of the system is conserved and that the phases share a common temperature at each pressure. The alternative model of allowing each phase to release along its own isentropic $P - T$ is negligibly different, as shown later. Given S held constant from the peak state and V on the $P - V$ release path, the mass fraction λ and T on the release path can be solved as described above. This calculation differs from the frozen-phase release calculations, where we used the same equations but held λ constant and solved for V; here, by contrast, we take V as given and compute λ.

[18] For release from H_1, stishovite might invert to quartz, amorphize, or melt. Let us first assume that only the stishovite-quartz transition occurs. We take the $P - V$ path H_1R literally and calculate the release $P - T$ path and mass fraction of stishovite (λ), as shown in Figures 6b and 3. Another possibility is that the phase change runs rapidly once it nucleates and that the $P - u_p$ data give an overly smoothed view of the transition, so we also calculate a two-step $P - V$ path that approximates H_1R (solid line) with H_1BR (Figure 6a) and redo the calculation for T and λ (Figures 6b and 3). There are only minor differences in temperature paths for these two cases; the estimated post-shock temperature for release to quartz is 1990 K using the Debye-Grüneisen model. At ambient pressure, tabulated data on heat capacity and entropy are available as well, and in this case the same temperature, 1990 K for quartz at 1 bar with the specific entropy of the H_1 Hugoniot state. The difference between this value for T_R and the post-shock temperature for the frozen-phase stishovite release from H_1, 2200 K, is comparable to the uncertainty in temperature measurement. In other words, the $P - u_p$ data clearly constrain the presence of phase changes on release but the post-shock temperature data do not.

[19] Release from H_2 and H_3 clearly involve crossing of the melting curve rather than formation of quartz. We need to consider whether this is best described as a melting process or an amorphization. In either case, stishovite loses its long-range order. Whether we describe states as liquid or amorphous depends on whether the disordered structure can continue to relax and maintain equilibrium configurations during release. This issue is conventionally addressed for relaxation of shear stresses by assuming a Maxwell-like viscoelastic rheology characterized by a shear modulus G and a temperature-dependent shear viscosity $\eta(T)$, in which case the characteristic relaxation time τ is given by $\tau = \eta(T)/G$. For silicate liquids, G is on the order of 10^{10} Pa. This viscosity describes shear relaxation but it is thought to approximate volume relaxation behavior as well. Thus, if we know the viscosity of the amorphous phase as a function of temperature, then for any given timescale of interest we can find a critical temperature T_g above which the system maintains relaxed states throughout the process and is deemed a liquid; otherwise, its density will be history-dependent and it is glass-like or simply amorphous. In this latter, unrelaxed case, there is the possibility of recovering a dense amorphous silica phase. At ambient pressure, the

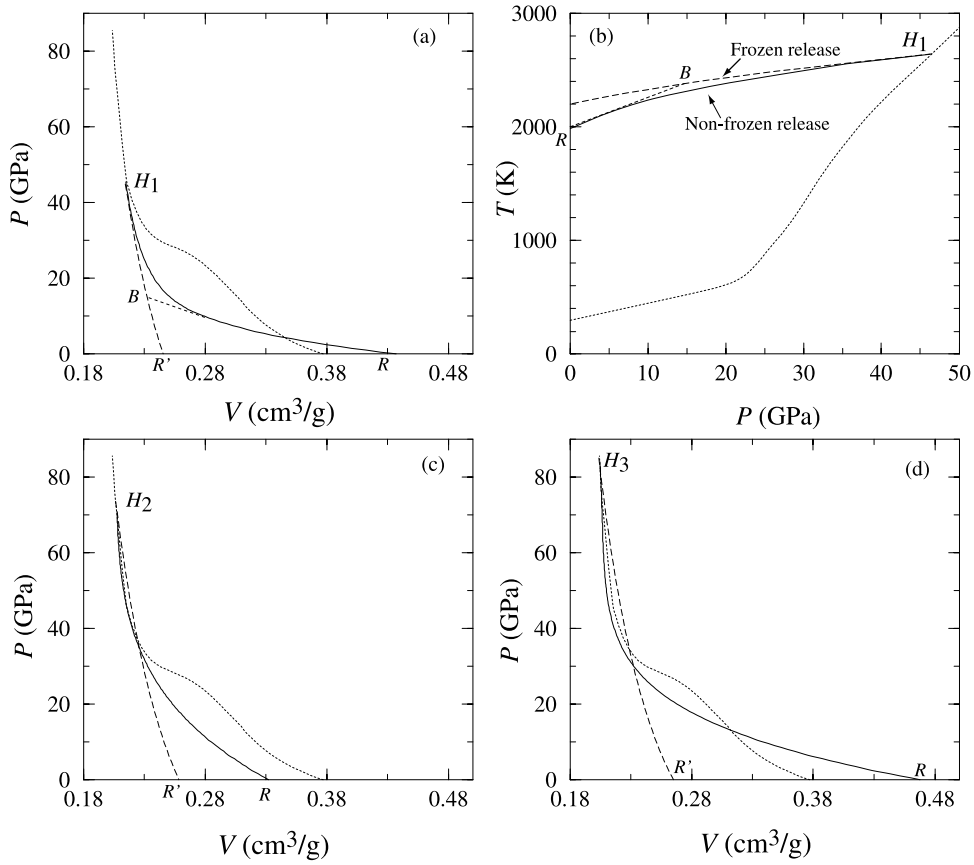

Figure 6. Principal Hugoniot of quartz (dotted curves), calculated frozen-release paths (long dashed curves), release paths converted from $P - u_p$ measurement [*Podurets et al.*, 1976] (solid curves) from shock states H_1 (*a*), H_2 (*c*), and H_3 (*d*), shown in $P - V$. For frozen release, the post-shock volume $V_{R'}$, $H_1 < H_2 < H_3$. For converted release path from $P - u_p$, $H_2 < H_1 < H_3$. In (*a*), B denotes a speculated stishovite-quartz transition point, and H_1BR is an approximation to solid curve H_1R. (b) The corresponding $P - T$ paths for H_1 with Hugoniot (dotted curve). Error bars are not available from *Podurets et al.* [1976], and the relative error for V is estimated as ~6% from *Chhabildas and Grady* [1984].

$\eta - T$ relationship of pure SiO_2, a strong liquid, can be described by an Arrhenius relationship [*Richet and Bottinga*, 1995],

$$\log \eta = -7 + A\left(\frac{10^4}{T}\right), \tag{16}$$

where constant $A \sim 2.67$, and η is in Pa · s. For the buffer method, the measured $P - u_p$ is an instantaneous value, and the release timescale involved is 10^{-9}–10^{-8} s. This is also the timescale over which release measurements probe the state of disordered stishovite. This indicates a critical temperature $T_g \sim 3100$ K. If the release time is larger, T_g will be even lower. In the case of H_2 and H_3, T_R of frozen release is higher than T_g; thus we describe the phase transition experienced by stishovite during release as melting and expect that the phase at the post-shock state will be low-density silica liquid. However, we cannot rule out unrelaxed decompression of a dense amorphous state during release because the above development makes several assumptions including a weak pressure-dependence of $\eta - T$ relationship, a constant shear modulus, and a similarity between volume and shear relaxation.

[20] Because the equation of state and thermodynamics of liquid silica at high P and T are poorly constrained, a meaningful and rigorous calculation of the complete release paths involving mixtures of stishovite/liquid or stishovite/glass will be left open. Entropy, heat capacity C_p, and thermal expansivities for stishovite and silica liquid at ambient pressure, however, are documented [*Malcolm*,

Table 3. Post-Shock ($P = 0$) Temperature for Isentropic Releases From Typical Peak Shock States[a]

Shock State	S_H, J/K/g	$T_{R,s}$, K	Phase Transition	V_R, cm^3/g	λ	$T_{R,m}$, K
H_1	2.768	2200	S → Q	0.4372	0	1990
H_1	2.768	2200	S → L	0.4372	0	1850
H_2	3.324	3200	S → L	0.3320	0.53	3110
H_3	3.543	3617	S → L	0.4676	0	3273

[a]Here *s* and *m* denote frozen and non-frozen release, respectively. For non-frozen case, phase changes of stishovite (S) to quartz (Q) and liquid (L) are considered. V_R is obtained from $P - u_p$ measurement (Figure 6), and λ is the mass fraction of stishovite and estimated with handbook values at ambient pressure.

1998; *Saxena et al.*, 1993; *Navrotsky*, 1994], and the above argument about relaxation time suggests that the liquid phase at the post-shock states released from H_2 and H_3 will be relaxed to low-pressure properties. Considering only the post-shock states at ambient pressure, then, knowledge of the entropy (presumed equal to shock state entropy) and the release volume V_R allows an estimate of the phase proportions and post-shock temperature after release from H_2R and H_3R (Table 3). In H_2 case, the mass fraction of stishovite is 0.53, and temperatures for frozen and non-frozen release differ by only 90 K. In H_3 case, stishovite transforms into liquid totally, and the post-shock temperature estimates are 3617 K and 3273 K for frozen and non-frozen release, respectively. Finally, if we now consider the possibility that the volume increase seen on release from H_1 is an amorphization rather than an inversion to quartz, the estimate of T_R from low-pressure properties of ordinary silica liquid suggests T_R = 1840 K (compared to 1990 K for inversion to quartz and 2200 K for frozen-phase stishovite). This is below the estimate of T_g for relaxed behavior, and so the liquid properties may not be appropriate. Nevertheless, it seems clear that in all cases, T_R estimates allowing for phase transitions during unloading are only 100–350 K lower than those for frozen release. Hence, without direct measurement of the phases present at release state, we can still conclude that the post-shock temperatures inferred by [*Boslough*, 1988] are approximately correct. Thus it appears to validate the methodology of measuring post-shock temperature [*Boslough*, 1988]. This also suggests that melting in SiO_2 upon release is best resolved from volume instead of temperature, because the entropy of fusion is too small to give a clear signal of T_R.

3. Discussion

3.1. Superheating

[21] In general, in studies of the kinetics of melting and freezing, it is straightforward to achieve undercooled liquid states but extremely challenging to obtain solids superheated above their congruent melting temperatures, mostly because of heterogeneous nucleation on grain boundaries and other sites. In shock loaded samples, however, temperatures can be increased by $\sim 10^3$ K on a ns timescale, corresponding to a heating rate of 10^{12} K/s. The sample is heated internally as the shock front passes, and hence superheating is limited by homogeneous nucleation. Shock temperature measurements on fused quartz and quartz [*Lyzenga et al.*, 1983] and sound speed measurements [*Chhabildas and Miller*, 1985] clearly demonstrate the persistence of stishovite above its melting curve and hence superheating upon shock loading. On the principal Hugoniot centered on quartz, the maximum superheating $(T - T_m)/T_m$ (where T_m is equilibrium melting temperature) is about 0.22 at ~110 GPa. If we examine the frozen release path with respect to the equilibrium phase boundary, the whole release path for H_3 is superheated. In the case of H_2, stishovite remains stable until the release path crosses the liquid-stishovite phase boundary at about 16 GPa, where stishovite becomes superheated. As shown in Figures 6c–6d, volume increases sharply below ~20 GPa along both release paths H_2R and H_3R. This could be associated with the sharp drop of T_m of stishovite beginning at 20 GPa (Figure 4), which gives rise to a rapid increase in the superheating ratio along these release paths below 20 GPa. In the case of H_3, superheating is about 0.1 at the shock state and increases to about 0.3 at 15 GPa, which appears to be similar to the homogeneous nucleation-limited maximum superheating in silica [*Luo et al.*, 2002c; *Luo and Ahrens*, 2003a, 2003b]. On the basis of the large volume attained by H_3 upon release, there appears to be sufficient time after nucleation occurs for the stishovite to melt completely. The case of H_2 is different in that the release state appears to be only partially molten despite being in the stability field of liquid. The explanation may lie in the very short time interval after the pressure (~2 GPa) at which the H_2 path achieves large superheating relative to its liquidus.

3.2. Polymorphism

[22] Polymorphism upon shock loading and unloading mainly involves quartz-stishovite transition and related mechanisms. During loading quartz transforms directly into stishovite (surpassing coesite) and the mixed-phase (quartz and stishovite) regime on the Hugoniot (15–46 GPa) lies at higher pressure than the equilibrium boundary. The rarity of recovered coesite in laboratory experiments on shocked quartz suggests that the forward and backward transitions between quartz and coesite are kinetically too sluggish to proceed during short shock durations [*Wackerle*, 1962]. The same may be true of the inverse transition of stishovite to coesite. However, the delayed onset of transition to stishovite upon loading implies that a special mechanism is needed to explain the common occurrence of this transition during shock loading. For quartz-stishovite transition, *Tan and Ahrens* [1990] proposed a combination of shear-band melting of quartz and recrystallization (progressive bond-bending model [*Stolper and Ahrens*, 1987]) as the quartz-stishovite transformation mechanism. The shear melting model follows *Grady* [1980], who suggested that heterogeneous strain concentrates deformation into narrow shear zones that can attain much higher temperature than that of the bulk sample. Stishovite is then thought to nucleate and grow from melt within the heated zones. Yet, since the heating mechanism depends on concentrating the deformation into a small fraction of the sample volume, it is unclear that a large mass fraction of the sample can be converted by such a mechanism until the bulk shock temperature begins to approach the melting curve. Hence this mechanism may explain minor conversion to stishovite but has difficulty explaining bulk transformation into stishovite near the high end of the mixed phase regime. The occurrence of lamellar features upon recovery can be explained by shear melting.

[23] An alternative (probably dominant) mechanism is a displacive transition from quartz to stishovite, involving a change in coordination number of Si from 4 to 6. Martensitic transition with coordination number change (from 6 to 8) has been found in B1-B2 transition in alkali halides [*Fraser and Kennedy*, 1973]. A possible displacive mechanism for quartz-stishovite transition, induced by uniform shear stress in the shocked sample, was suggested by *Podurets et al.* [1976]. Besides kinetic effect, we speculate that the presence of non-hydrostatic stress could shift the phase boundary [*Simha and Truskinovsky*, 1994] toward higher pressures relative to the hydrostatic equilibrium. This mechanism can explain the occurrence of the quartz-stishovite transition when quartz-coesite is not observed,

its occurrence at higher pressure than expected, and its ability to achieve bulk transformation to stishovite well below the melting curve. We also note that this may explain the curious observation that upon release from H_1 and H_2, the reverse transformation seems to occur before the phase boundary is crossed, which the model of kinetic delay of a phase transition (until a certain driving force is developed due to overpressure or underpressure) cannot explain. That is, since displacive transitions are in general reversible, the back transition may be taking place under non-hydrostatic conditions. Hence we prefer the model of displacive transition of quartz to stishovite, perhaps with a minor role for shear melting.

3.3. Amorphization

[24] There have been numerous observations of formation of amorphous phases upon compression and decompression at low temperature, sometimes termed cold melting. A similar mechanism has been proposed for the increase in density by formation of a dense amorphous phase through the mixed phase regime (15–46 GPa) along the principal Hugoniot of quartz studies [*Sharma and Sikka*, 1996; *Chaplot and Sikka*, 2000] which we are here attributing to formation of crystalline stishovite, although amorphization on Hugoniot cannot be ruled out as a possibility.

[25] Proposals for the mechanism of cold melting [*Hemley et al.*, 1988; *Richet and Gillet*, 1997] involve the relative transformation kinetics of solid-solid phase changes and solid-amorphous changes. That is, although crystal I persists metastably in the stability field of crystal II, upon crossing of the metastable extension of the melting curve of crystal I the amorphization process may be kinetically easier than the solid-solid transition. Ice and silica are two classical examples of pressure-induced amorphization. Hexagonal H_2O ice (I_h) transforms into high density amorphous ice (*hda*) at about 1 GPa and 77 K [*Mishima et al.*, 1984]. *Hemley et al.* [1988] demonstrated that at room temperature, crystalline silica (quartz or coesite) becomes amorphous between 25–35 GPa. The insert to Figure 4 illustrates the process and its relationship to metastable melting curves with silica as an example. With static compression at room temperature (the dotted arrow), quartz and coesite are expected to transform to stishovite beginning at below 10 GPa. Instead, the low-pressure solid persists to 25–35 GPa and then amorphizes. This is the pressure range where the fictitious melting temperatures on the metastable extensions of the melting curves of quartz (EQ) and coesite (EC) may cross below 300 K. Thus quartz and coesite transform to dense amorphous silica instead of stishovite. The underlying assumption is that amorphization of quartz and coesite are kinetically favored relative to transition to stishovite, at the timescale of static experiments. During shock compression, however, there are several factors that may kinetically favor solid-solid transition. First, the present calculation shows that at 25–35 GPa, the temperature is in the range of 850–1900 K, where transition kinetics should be much faster than at 300 K. Second, the non-hydrostatic stress conditions may allow a displacive martensitic transition mechanism at the shock front. In part. the notion that shock compression forms a dense amorphous phase is based on recovery experiments [*Gratz et al.*, 1992; *Sharma and Sikka*, 1996; *Fiske et al.*, 1998], but recovered amorphous material may well have formed during or after release. The excellent match between the Hugoniot equation of state of silica and static high pressure data on stishovite argue for stishovite-like phase on the Hugoniot [*Luo et al.*, 2002a], and solid-solid transition is kinetically plausible. While there is no direct evidence ruling out amorphization on Hugoniot, the recovery of non-negligible amount of stishovite (and other crystalline phases such as Fe_2N-type) [*De Carli and Milton*, 1965; *Kleeman and Ahrens*, 1973; *Sekine et al.*, 1987] supports the hypothesis that pure stishovite or a crystalline stishovite-like phase indeed occurs in the Hugoniot state.

[26] On the basis of logic similar to that invoked for cold pressure-induced amorphization, *Richet* [1988] proposed the possibility of amorphization upon decompression across metastable extensions of the melting curves of high-pressure phases. As shown in the insert to Figure 4, we drew a fictitious metastable extension of stishovite melting (ES) into the low-pressure regime which intersects the *T*-axis at about 900 K. Thus, if the post-shock temperature is higher than 900 K, stishovite could transform to a dense amorphous phase (diaplectic glass) upon release [*Skinner and Fahey*, 1963]. Similar behavior is observed on decompression of other silicates such as $CaSiO_3$ perovskite [*Liu and Ringwood*, 1975]. This may be part of the reason that stishovite is rarely recovered. Even though we argue that stishovite does form at the shock state, in order to be recovered it would have to survive amorphization, inversion to quartz, and ordinary thermal melting during release and cooling.

3.4. Isentropic Assumption Upon Release

[27] In the above discussion of release from shock states, we assumed isentropic paths. This assumption produced sensible results, for example, the calculated post-shock temperature agrees with measurement and, as we will see below, is consistent with recovery results. However, we do not have independent verification. Thus it is necessary to examine the maximum entropy production possible as shown in the following cases.

[28] First, we compare the frozen-phase release of a two-phase aggregate in which the phases maintain thermal equilibrium to the case where each phase follows its own isentrope and then they return to thermal equilibrium at 1 bar. We will take release from $P_H = 35.8$ GPa ($S_H = 2.393$ J/K/g, $T_H = 1900$ K, mass fraction of stishovite $\lambda_H = 0.82$) as a typical example. If as above we assume that quartz and stishovite maintain thermal equilibrium upon release, then $T_R = 1710$ K is common to both phases. Now we let quartz and stishovite release separately and isentropically from the shock state with specific entropy of each phase and mass fractions fixed, and the post shock temperatures are different (1466 K and 1772 K for quartz and stishovite, respectively). If the system returns to thermal equilibrium at $P = 0$, the maximum entropy production for this adiabatic isobaric process will be the isenthalpic case. The total enthalpy of the system can be readily calculated at post-shock state. If we assume that mass fractions of the phases at final state continue to remain constant, we obtain $T_h = 1720$ K (compared to $T_R = 1710$ K) and the entropy production is negligible.

[29] If in the above case we let the phase proportions change as well during the isenthalpic step at ambient

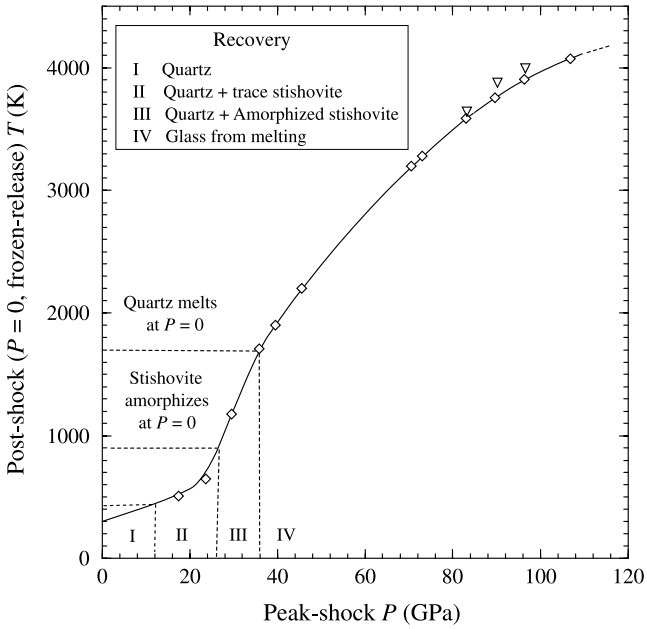

Figure 7. Frozen-phase release post-shock temperature versus peak-state shock pressure. Diamonds: calculated; inverted triangles, measurements [*Boslough*, 1988]. The regimes of different recovery phases are indicated (also see Table 4).

pressure, the maximum entropy is produced when the mass fraction of quartz goes to 1, which corresponds to $T_h = 2240$ K and a significant entropy increase of 22% relative to S_H. This is an extreme case since we delayed the phase transition all the way to ambient pressure, but it implies that phase transitions that occur during release but with finite driving force could significantly increase the entropy. We presently lack a formalism for rigorously evaluating such cases because the Riemann invariant formulation, equation (15), assumes isentropic flow and is no longer applicable. Despite this uncertainty, however, our calculations based on isentropic assumption appear to yield reasonable results. Thus we regard release involving phase changes as a quasi-isentropic process, and isentropic assumption is at least acceptable to first order.

4. A Pressure-Temperature Scale

[30] The principal Hugoniot of quartz can be divided into distinct regimes of pressure based on the phases present at peak shock state: 0–15 GPa, quartz; 15–46 GPa, mixture of quartz and stishovite; 46–77 GPa, stishovite; 77–110 GPa, superheated metastable stishovite; >110 GPa, melt. Here we use our calculations of temperature and phases at post-shock states calculated by frozen-phase isentropic release to predict recovery products that will survive after cooling to ambient temperature, assuming cooling slow enough to avoid quenching of the post-shock phases, as shown in Figure 7. At ambient pressure, stishovite become amorphous as low as 800–950 K [*Skinner and Fahey*, 1963; *Brazhkin et al.*, 1991], the release temperature corresponding to peak shock pressure of ~26 GPa. Quartz melts metastably at 1700 K (expected upon release from peak shock pressure of 35 GPa). Thus, given the mass fractions of quartz and stishovite at peak-shock state, the post-shock temperature from frozen release and phase stability, we divide peak-shock pressure into four regimes (Figure 7), distinct from the five shock-state regimes: 1. P_H = 0–15 GPa, T_R = 300–450 K and Recovery = quartz. Along Hugoniot, no quartz transforms into either coesite or stishovite, due to sluggish quartz-coesite transformation rate and low temperatures. Thus only quartz will be recovered. 2. P_H = 15–26 GPa, T_R = 450–900 K, and Recovery = quartz + trace stishovite. Stishovite with mass fraction of up to 0.25 is produced on Hugoniot, and T_R is lower than 900 K. Stishovite will not amorphize, but the back-transformation to quartz is fast. Thus only trace stishovite will be recovered. 3. P_H = 26–36 GPa, T_R = 900–1700 K, and Recovery = quartz + dense amorphous glass. In this case, significant stishovite (λ =0.25–0.8) is produced at shock state. Even if stishovite did not invert to quartz, it would amorphize with density higher than ordinary silica glass. Quartz will not melt metastably or transform to tridymite due to slow kinetics. Thus only quartz and dense amorphous glass can be recovered. The latter could be diaplectic glass. 4. P_H > 36 GPa, T_R > 1700 K and Recovery = ordinary glass. Both stishovite and quartz (no matter what the mass fraction is at post-shock state) will melt and ordinary glass formed from silica melt is the only phase in recovery. We summarized in Table 4 the above results as a pressure-temperature scale for impact events involving quartz.

[31] In the above discussion, we assumed frozen-phase release, which is not necessarily true for all pressures. We already demonstrated that T_R from non-frozen phase release is slightly lower than T_R in frozen release (Table 3), and it will not change our results. The above analysis indicates that shock recovery of a large fraction of stishovite is essentially impossible, as predicted by *Skinner and Fahey* [1963], although some stishovite can be recovered by special experiment design [e.g., *Kleeman and Ahrens*, 1973]. Shear melting related phenomena (e.g., lamellar features) could be present in low-pressure recovery (e.g., cases 2 and 3), but they are not dominant and are second-order features. To first order, we can apply the pressure-temperature scale from frozen-phase release to impact

Table 4. A Pressure-Temperature Scale for Impact Events Involving Quartz

	Shock			Release		
	P_H, GPa	T_H, K	Phases on Hugoniot	P_H, GPa	T_R, K	Phases Recovered
I	0–15	300–500	quartz	0–15	300–450	quartz
II	15–46	500–2600	quartz, stishovite	15–26	450–900	quartz, trace stishovite
III	46–77	2600–4700	stishovite	26–36	900–1700	quartz, diaplectic glass
IV	77–110	4700–6850	superheated stishovite	>36	>1700	ordinary glass
V	>110	>5000	melt	–	–	–

events involving quartz. Interestingly, despite careful consideration here of the kinetics and stability of many possible phases, our results are not dramatically different from *Stöffler* [1971] based on earlier calculations of shock and post-shock temperature [*Wackerle*, 1962]. As shown next, predictions with our scale (Table 4 and Figure 7) agree well with recovery experiments.

[32] Many recovery experiments have been conducted on silica. Recovered material from quartz shock loaded to 60 GPa is amorphous with density of ordinary silica [*De Carli and Jamieson*, 1959], indicating glass formed from melting as predicted by our calculation. At 35 GPa, recovered material has density of 2.64 g/cm^3 and broadened X-ray peaks of α-quartz [*De Carli and Jamieson*, 1959], consistent with a small fraction of dense amorphous silica. Similarly, *De Carli and Milton* [1965] recovered predominantly quartz with minor short-range-order (SRO) (possibly due to minor shear melting) and trace stishovite at 14–16 GPa (at 16 GPa, we predict 2% stishovite is formed at shock). From 25 Gpa, *Wackerle* [1962] recovered essentially quartz, and from about 50 GPa, ordinary glass with density 2.2 g/cm^3.

[33] This work demonstrates that the phases recovered are not necessarily the same as those at post-shock state or peak shock state. While the shock state and release path are constrained with confidence, the phase changes between recovery and post-shock state are not. This part of the process depends on size-dependent sample-environment interaction, particularly heat conduction to the surroundings. For example, the temperature of the post-shock state upon release of shocked quartz from $P_H = 70$ GPa suggests complete post-shock melting and recovery of ordinary glass. However, there is a narrow range near our example H_2 where the post-shock state includes stishovite which might, with a rapid enough quench, be recoverable. Furthermore, in the interpretation of recovered samples from natural impacts, porosity and impurities such as water content need also be taken into account.

5. Conclusion

[34] We computed the thermodynamic states along the principal Hugoniot (including mixed-phase regime) of quartz and frozen-phase release paths based on classical Debye-Grüneisen theory, and quantified the phases, mass fractions, and temperatures. Along the Hugoniot, quartz converts to stishovite-like phase in the range 15–46 GPa. Superheating of stishovite-like phase along the Hugoniot between 77–110 GPa is confirmed. Comparison to the phase diagram of silica shows that the frozen release paths may enter the stability fields of quartz or liquid, and cross the metastable (cold) melting curve of stishovite, suggesting that releases may not maintain frozen phase assemblages. This is supported by $P - V$ release paths converted from measurements on $P - u_p$ assuming isentropic release. Shock temperature and post-shock temperature calculations with frozen or non-frozen release yielded values in accord with shock and post-shock temperature measurements. This validates the method of measuring post-shock temperature but shows the poor sensitivity of such measurements to phase transitions during decompression compared to volume information, at least for silica. The isentropic assumption appears to yield useful first-order results even for non-frozen release.

[35] The phase proportions in the computed Hugoniot states and the frozen-phase release temperatures provide an appropriate pressure-temperature scale for impact events involving quartz. It is necessary to distinguish recovered phases and phases produced upon shock loading and unloading. The proposed scale is consistent with previous shock recovery experiments and demonstrates that while recovery of trace quantities of crystalline stishovite-like phase is straightforward, the recovery of a large quantity of such phase from shock loading on quartz does not occur without special quenching mechanisms.

[36] **Acknowledgments.** S.-N. Luo has been supported by NSF grant EAR-0207934. We appreciate helpful discussions with Z. R. Wang, D. Andrault, and O. Tschauner. Comments by I. Jackson and two reviewers helped improve the manuscript. Contribution 8916, Division of Geological and Planetary Sciences, California Institute of Technology.

References

Ahrens, T. J., and J. V. G. Gregson, Shock compression of crustal rocks: Data for quartz, calcite, and plagioclase rocks, *J. Geophys. Res.*, *69*, 4839–4874, 1964.

Ahrens, T. J., and J. T. Rosenberg, Shock metamorphism: Experiments on quartz and plagioclase, in *Shock Metamorphism of Natural Materials*, edited by B. M. French and N. M. Short, pp. 59–81, MonoBook Corp., Baltimore, Md., 1968.

Ahrens, T. J., C. F. Petersen, and J. T. Rosenberg, Shock compression of feldspar, *J. Geophys. Res.*, *74*, 2727–2746, 1969.

Akins, J. A., Dynamic compression of minerals in the MgO-FeO-SiO_2 system, Ph.D. thesis, California Institute of Technology, Pasadena, Calif., 2003.

Akins, J. A., and T. J. Ahrens, Dynamic compression of SiO_2: A new interpretation, *Geophys. Res. Lett.*, *29*, 1394, doi:10.1029/2002GL014806, 2002.

Al'tshuler, L. V., R. F. Trunin, and G. V. Simakov, Shock wave compression of periclase and quartz and the composition of the Earth's lower mantle, *Izv. Akad. Nauk USSR, Fiz. Zemli*, *10*, 1–6, 1965.

Anderson, O. L., A simplified method for calculating the Debye temperature from elastic constants, *J. Phys. Chem. Solids*, *24*, 909–917, 1963.

Boettger, J. C., New model for the shock-induced α-quartz $\rightarrow$ stishovite transition, *J. Appl. Phys.*, *72*, 5500–5508, 1992.

Boslough, M. B., Postshock temperatures in silica, *J. Geophys. Res.*, *93*, 6477–6484, 1988.

Brazhkin, V. V., R. N. Voloshin, and S. V. Popova, The kinetics of the transition of metastable phases of SiO_2, stishovite and coesite to the amorphous state, *J. Non Cryst. Solids*, *136*, 241–248, 1991.

Chaplot, S. L., and S. K. Sikka, Molecular-dynamics simulation of shock-stress-induced amorphization of α-quartz, *Phys. Rev. B*, *61*, 11,205–11,208, 2000.

Chhabildas, L. C., and D. E. Grady, Dynamic material response of quartz at high strain rates, *Mater. Res. Soc. Symp. Proc.*, *22*, 147–150, 1984.

Chhabildas, L. C., and J. M. Miller, Release-adiabat measurements in crystalline quartz, *Sandia Rep. SAND85-1092*, Sandia Natl. Lab., Albuquerque, N. M., 1985.

Cohen, R. E., R. E. Gülseren, and R. J. Hemley, Accuracy of equation-of-state formulations, *Am. Mineral.*, *85*, 338–344, 2000.

Cordier, P., J. C. Doukhan, and J. Peyronneau, Structural transformations of quartz and berlinite $AlPO_4$ at high pressure and room temperature: A transmission electron-microscopy study, *Phys. Chem. Miner.*, *20*, 176–189, 1993.

De Carli, P. S., and J. C. Jamieson, Formation of an amorphous form of quartz under shock conditions, *J. Chem. Phys.*, *31*, 1675–1676, 1959.

De Carli, P. S., and D. J. Milton, Stishovite, synthesis by shock wave, *Science*, *165*, 144–145, 1965.

Dera, P., C. T. Prewitt, N. Z. Boctor, and R. J. Hemley, Characterization of a high-pressure phase of silica from the Martian Shergotty, *Am. Mineral.*, *87*, 1018–1023, 2002.

Dubrovinsky, L. S., N. A. Dubrovinskaia, S. K. Saxena, T. Tutti, S. Rekhi, T. Le Bihan, G. Shen, and J. Hu, Pressure induced transformations of cristobalite, *Chem. Phys. Lett.*, *333*, 264–270, 2001.

Fiske, P. S., W. J. Nellis, Z. Xu, and J. F. Stebbins, Shocked quartz: A Si-29 magic-angle-spinning nuclear magnetic resonance study, *Am. Mineral.*, *83*, 1285–1292, 1998.

Fraser, W. L., and S. W. Kennedy, The crystal-structural transformation NaCl-type → CsCl-type: Analysis by Martensite theory, *Acta Crystallogr., Sect. A*, *30*, 13–22, 1973.

Grady, D. E., Shock deformation of brittle solids, *J. Geophys. Res.*, *85*, 913–914, 1980.

Grady, D. E., W. J. Murri, and G. R. Fowles, Quartz to stishovite: Wave propagation in the mixed phase region, *J. Geophys. Res.*, *79*, 332–338, 1974.

Gratz, A. J., W. J. Nellis, J. M. Christine, W. Brocious, J. Swegle, and P. Cordier, Shock metamorphism of quartz with initial temperatures −170°C to 1000°C, *Phys. Chem. Minerals*, *19*, 267–288, 1992.

Haines, J., J. M. Leger, F. Gorelli, and M. Hanfland, Crystalline post-quartz phase in silica at high pressure, *Phys. Rev. Lett.*, *87*, doi:10.1103/PhysRevLett.87.155503, 2001.

Hemley, R. J., A. P. Jephcoat, H. K. Mao, L. C. Ming, and M. H. Manghnani, Pressure-induced amorphization of crystalline silica, *Nature*, *334*, 52–54, 1988.

Hemley, R. J., C. T. Prewitt, and K. J. Kingma, High-pressure behavior of silica, *Rev. Mineral.*, *29*, 41–81, 1994.

Karki, B. B., L. Stixrude, and J. Crain, Ab initio elasticity of three high-pressure polymorhs of silica, *Geophys. Res. Lett.*, *24*, 3269–3292, 1997.

Kleeman, J. D., and T. J. Ahrens, Shock-induced transition of quartz to stishovite, *J. Geophys. Res.*, *78*, 5954–5960, 1973.

Langenhorst, F., A. Deutsch, D. Stöffler, and U. Hornemann, Effect of temperature on shock metamorphism of single-crystal quartz, *Nature*, *356*, 507–509, 1992.

Liu, L.-G., and A. E. Ringwood, Synthesis of a perovskite-type polymorph of $CaSiO_3$, *Earth Planet. Sci. Lett.*, *28*, 209–211, 1975.

Loveridge-Smith, A., et al., Anomalous elastic response of silicon to uniaxial shock compression on nanosecond time scales, *Phys. Rev. Lett.*, *86*, 2349–2352, 2001.

Luo, S.-N., and T. J. Ahrens, Superheating systematics of crystalline solids, *Appl. Phys. Lett.*, *82*, 1836–1838, 2003a.

Luo, S.-N., and T. J. Ahrens, Shock-induced superheating and melting curves of geophysically important minerals, *Phys. Earth Planet. Lett.*, in press, 2003b.

Luo, S.-N., J. L. Mosenfelder, P. D. Asimow, and T. J. Ahrens, Direct shock wave loading of stishovite to 235 GPa: Implications for perovskite stability relative to an oxide assemblage at lower mantle conditions, *Geophys. Res. Lett.*, *29*, 1691, doi:10.1029/2002GL015627, 2002a.

Luo, S.-N., T. Cagin, A. Strachan, W. A. Goddard III, and T. J. Ahrens, Molecular dynamics modeling of stishovite, *Earth Planet. Sci. Lett.*, *202*, 147–157, 2002b.

Luo, S.-N., T. J. Ahrens, T. Cagin, A. Strachan, and W. A. Goddard III, Superheating of crystalline solids: Theory, experiment, simulation, and application to static and dynamic high-pressure melting, *EOS Trans. AGU*, *83*(47), Fall Meet. Suppl., MR62B-1080, 2002c.

Lyzenga, G. A., and T. J. Ahrens, The relation between the shock-induced free-surface velocity and the postshock specific volume of solids, *J. Appl. Phys.*, *49*, 201–204, 1978.

Lyzenga, G. A., T. J. Ahrens, and A. C. Mitchell, Shock temperatures of SiO_2 and their geophysical implications, *J. Geophys. Res.*, *88*, 2431–2444, 1983.

Malcolm, W. C., Jr., *NIST-JANAF Thermochemical Tables*, Am. Chem. Soc. and Am. Inst. of Phys. for the Natl. Inst. of Standards and Technol., Gaithersburg, Md., 1998.

Marsh, S. P., *LASL Shock Hugoniot Data*, pp. 321–324, Univ. of Calif. Press, Berkeley, Calif., 1981.

Mishima, O., L. D. Calvert, and E. Whalley, Melting of Ice-I at 77-K and 10-Kbar—A new method of making amorphous solids, *Nature*, *310*, 393–395, 1984.

Morse, P. M., *Thermal Physics*, Benjamin, White Plains, N. Y., 1964.

Murakami, M., K. Hirose, S. Ono, and Y. Ohishi, Stability of $CaCl_2$-type and α-PbO_2-type SiO_2 at high pressure and temperature determined by in-situ X-ray measurements, *Geophys. Res. Lett.*, *30*, 1207, doi:10.1029/22002GL016722, 2003.

Navrotsky, A., Thermochemistry of silica, *Rev. Mineral.*, *29*, 309–329, 1994.

Ng, A., B. K. Godwal, J. Waterman, L. DaSilva, N. W. Ashcroft, and R. Jeanloz, Nonequilibrium shock behavior in quartz, *Phys. Rev. B*, *44*, 4872–4876, 1991.

Panero, W. R., L. R. Benedetti, and R. Jeanloz, Equation of state of stishovite and interpretation of SiO_2 shock-compression data, *J. Geophys. Res.*, *108*, 2015, doi:10.1029/2001JB001663, 2003.

Podurets, M. A., G. V. Simakov, and R. F. Trunin, On the phase equilibrium in shock-compressed quartz and on the kinetics of phase transitions, *Izv. Earth Phys.*, *12*, 419–424, 1976.

Podurets, M. A., G. V. Simakov, G. S. Telegin, and R. F. Trunin, Polymorphism of silica in shock waves and equation of state of coesite and stishovite, *Izv. Acad Sci. USSR Phys. Solid Earth*, *17*, 9–15, 1981.

Richet, P., Superheating, melting, and vitrification upon decompression of high-pressure minerals, *Nature*, *331*, 56–58, 1988.

Richet, P., and Y. Bottinga, Rheology and configurational entropy of silicate melts, in, *Rev. Mineral.*, *32*, 67–93, 1995.

Richet, P., and P. Gillet, Pressure-induced amorphization of minerals: A review, *Eur. J. Mineral.*, *9*, 907–933, 1997.

Robie, R. A., B. S. Hemingway, and J. R. Fisher, *Thermodynamic Properties of Minerals and Related Substances at 298.15K and 1 Bar (105 Pascals) Pressure and at Higher Temperatures*, U.S. Govt. Print. Off., Washington, D. C., 1978.

Saxena, S. K., N. Chatterjee, Y. Fei, G. Shen, *Thermodynamic Data on Oxides and Silicates*, Springer-Verlag, New York, 1993.

Sekine, T., M. Akaishi, and N. Setaka, Fe_2N-type SiO_2 from shocked quartz, *Geochim. Cosmochim. Acta*, *51*, 379–381, 1987.

Sharma, S. M., and S. K. Sikka, Pressure induced amorphization of materials, *Prog. Mater. Sci.*, *40*, 1–77, 1996.

Shen, G. Y., and P. Lazor, Measurement of melting temperatures of some minerals under lower mantle pressures, *J. Geophys. Res.*, *100*, 17,699–17,713, 1995.

Simha, N., and L. Truskinovsky, Shear-induced transformation toughening in ceramics, *Acta Metall. Mater.*, *42*, 3827–3836, 1994.

Skinner, B. J., and J. J. Fahey, Observations on the inversion of stishovite to silica glass, *J. Geophys. Res.*, *68*, 5595–5604, 1963.

Stöffler, D., Progressive metamorphism and classification of shocked and breciated crystalline rocks at impact craters, *J. Geophys. Res.*, *76*, 5541–5551, 1971.

Stolper, E. M., and T. J. Ahrens, On the nature of pressure-induced coordination changes in silicate melts and glasses, *Geophys. Res. Lett.*, *14*, 1231–1233, 1987.

Swegle, J. W., Irreversible phase transitions and wave propagation in silicate geologic materials, *J. Appl. Phys.*, *68*, 1563–1579, 1990.

Tan, H., and T. J. Ahrens, Shock-induced polymorphic transition in quartz, carbon, and boron nitride, *J. Appl. Phys.*, *67*, 217–224, 1990.

Trunin, R. F., G. V. Simakov, M. A. Podurets, B. N. Moiseyev, and L. V. Popov, Dynamic compressibility of quartz and quartzite at high pressure, *Izv. Acad Sci. USSR Phys. Solid Earth*, *1*, 8–11, 1971.

Wackerle, J., Shock-wave compression of quartz, *J. Appl. Phys.*, *33*, 922–937, 1962.

Zel'dovich, Y. B., and Y. P. Raizer, *Physics of Shock Waves and High-Temperature Hydrodynamic Phenomena*, Dover, Mineola, N. Y., 2002.

Zhugin, Y. N., K. K. Krupnikov, N. P. Voloshin, and Y. A. Shoidin, Phase transformations in quartz, induced by shock waves from underground nuclear explosions, *Izv. Acad Sci. USSR Phys. Solid Earth*, *35*, 478–483, 1999.

T. J. Ahrens, Lindhurst Laboratory of Experimental Geophysics, Seismological Laboratory, California Institute of Technology, Pasadena, California, USA. (tja@gps.caltech.edu)

P. D. Asimow, Division of Geological and Planetary Sciences, California Institute of Technology, Pasadena, CA 91125, USA. (asimow@gps.caltech.edu)

S.-N. Luo, Plasma Physics P-24, MS E526, Los Alamos National Laboratory, Los Alamos, NM 87545, USA. (sluo@lanl.gov)